

Experimental Investigation and Optimization of Nanoparticle Mass Concentration and Heat Input of Loop Heat Pipe

P. Gunnasegaran, M. Z. Abdullah, M. Z. Yusoff, Nur Irmawati

Abstract—This study presents experimental and optimization of nanoparticle mass concentration and heat input based on the total thermal resistance (R_{th}) of loop heat pipe (LHP), employed for PC-CPU cooling. In this study, silica nanoparticles (SiO_2) in water with particle mass concentration ranged from 0% (pure water) to 1% is considered as the working fluid within the LHP. The experimental design and optimization is accomplished by the design of experimental tool, Response Surface Methodology (RSM). The results show that the nanoparticle mass concentration and the heat input have significant effect on the R_{th} of LHP. For a given heat input, the R_{th} is found to decrease with the increase of the nanoparticle mass concentration up to 0.5% and increased thereafter. It is also found that the R_{th} is decreased when the heat input is increased from 20W to 60W. The results are optimized with the objective of minimizing the R_{th} , using Design-Expert software, and the optimized nanoparticle mass concentration and heat input are 0.48% and 59.97W, respectively, the minimum thermal resistance being 2.66 ($^{\circ}\text{C}/\text{W}$).

Keywords—Loop heat pipe, nanofluid, optimization, thermal resistance.

I. INTRODUCTION

LOOP HEAT PIPE (LHP) is a simple device used to transfer the heat from one place to the other. The advantage of using a LHP over the other ordinary methods to heat transfer is that the LHP can have an extremely high thermal conductance in steady state operation, and hence known as “super thermal conductors”. A typical LHP consists of five parts, including the evaporator, the compensation chamber, the vapor line, the condenser, and the liquid line. The heat is transferred as latent heat energy by evaporating the working fluid in the evaporator (hot side) and condensing the vapor in the condenser (cool side), the circulation is completed by the forces, such as capillary force or pump force directly acting on the liquid. The traditional shape of the evaporator is cylinder, and it is thought that a flat evaporator can reduce the thermal resistance between the evaporator and the heat source

[1]. Regardless of the classifications of LHPs, which might depend on the geometries, applications, and so on, the basic principles are the same.

Nowadays electronics and computers are quite a promising sphere of LHPs application. Computer technology, in particular PC “Notebook”, is a new sphere of LHPs application, which was revealed owing to the appearance of miniature and fairly efficient devices. It is intended for the PC “Notebook” with a processor Athlon XP, which at a maximum loading dissipates about 70W. By predictions of experts, in the near future one can expect the appearance of more powerful processors dissipating 100W and more [2]. Based on these applications, “lightweight” and “high performance” becomes the key goals for current LHP design, for application in the electronic industries. Normally, conventional fluids are used in LHPs to remove the heat based on a temperature range for its particular operating conditions. The lower thermal conductivity of these working fluids limits the thermal performance enhancement of the LHPs. Fluid, with nanoparticles is referred to as nanofluid, a term proposed by Choi [3]. The term ‘nanofluid’ refers to a two-phase mixture with its continuous phase being generally a liquid and the dispersed phase constituted of ‘nanoparticles’ i.e., extremely fine metallic particles of size below 100 nm. In other words, the large surface-area-to volume ratio also increases the stability of the suspensions. Since the 1995, researchers began to apply nanofluids in heat transfer devices, and have achieved many meaningful results on heat transfer enhancement. Thus, the nanofluid is a promising heat transfer fluid in variety of applications.

Recently, many researchers have presented the heat transfer characteristics of heat pipe using nanofluids. In contrast, the fundamental studies of nanofluids applied in heat pipes are still in its initial stage. Most of which are experimental study considered on conventional heat pipes such as micro-grooved heat pipe, mesh wick heat pipe, and oscillating heat pipe, and there is far less work conducted for LHPs. Some experimental results cannot be unified yet. Moreover, study on optimization of operating parameters, which are heat input power and nanoparticle mass concentrations is also rare. The theoretical investigations on nanofluids in heat pipes are very few [4]-[6] and hence validating the experimental findings is difficult. Accordingly, in the present study, the application of nanofluid in LHP is addressed experimentally and the results are optimized with the objective of minimizing the total thermal resistance of LHP charged with nanofluid, using Design-

P. Gunnasegaran is with the Centre for Fluid Dynamics (CFD), College of Engineering, Universiti Tenaga Nasional, Putrajaya Campus, Jalan IKRAM-UNITEN, 43000 Kajang, Malaysia (corresponding author: +603+89212230; fax: +603+89212116; e-mail: prem@uniten.edu.my).

M. Z. Abdullah is with the School of Mechanical Engineering, Universiti Sains Malaysia, Engineering Campus, 14300 Nibong Tebal, Penang, Malaysia (e-mail: mezul@eng.usm.my).

M. Z. Yusoff and Nur Irmawati are with the Centre for Fluid Dynamics (CFD), College of Engineering, Universiti Tenaga Nasional, Putrajaya Campus, Jalan IKRAM-UNITEN, 43000 Kajang, Malaysia (e-mail: zamri@uniten.edu.my and irmawati@uniten.edu.my).

Expert software.

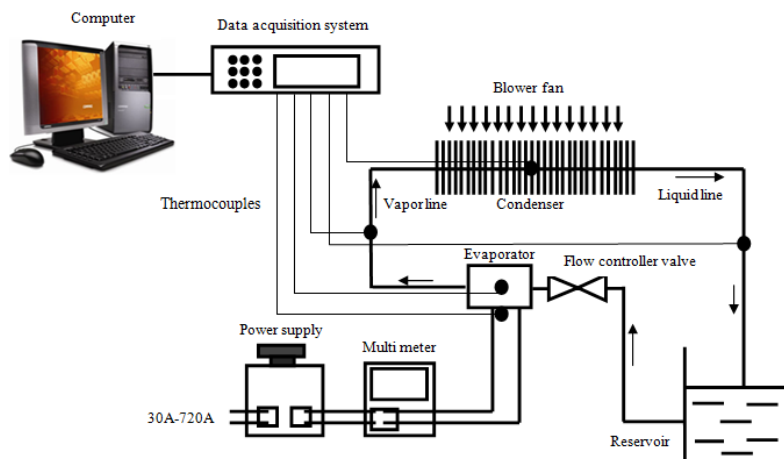


Fig. 1 Schematic diagram of experimental apparatus

II. MATERIALS AND METHODS

A. The Experimental Setup

The schematic diagram of experimental setup for LHP under investigation is shown in Fig. 1. The main function of this experiment rig is to determine the thermal performance of LHP charged with $\text{SiO}_2\text{-H}_2\text{O}$ nanofluid with mass concentration ranged from 0%-1% as a working fluid. The LHP shown in Fig. 1 installed with a power supply (W5 Series 30A-720A) and a flat evaporator, which is combined with the compensation chamber, with a total dimension of $50\text{ mm} \times 50\text{ mm} \times 4\text{ mm}$. A water tank with 0.75 liter glass vessel equipped by drain valve is used as liquid reservoir. The whole LHP is made of copper. The internal and external diameters of both vapor and liquid lines are 13.5 mm and 15 mm, respectively. The condenser section is made of 50 aluminum rectangular fins and cooled by installing two pieces of long screwed fans. To maintain steady state cooling conditions in the condenser section, the temperature and flow rate of the cooling liquid are fixed at constant value. The vacuum is maintained in the heat pipe by heating the tube at the evaporator section and the impurities are removed by opening the pressure release valve. To minimize the heat loss, the whole LHP is insulated by using glass wool. A copper block with heat rods inside is used to simulate the heat source, and the contact area between the evaporator and the heat source is $50\text{ mm} \times 50\text{ mm}$. In this experiment, the K-type thermocouples are installed on the pipe/wall in different locations of the loop, including the copper base plate (T_b), the evaporator (T_e), the vapor line (T_v), the condenser section (T_c) and the liquid line (T_l). The temperatures measured by the thermocouples are collected through a data acquisition (Agilent 34970A) with sample rate of 1 Hz and connected to a PC to collect the data. The experiments are conducted under a heat input ranged from 20W to 60W. The airflow velocity is fixed as 4 m/s and the coolant flow rate is 750 liters per hour, controlled by adjusting the flow control valve. The specifications of the LHP are listed in Table I.

B. Nanofluid Preparation

In the present study, deionized water is used as the base liquid for preparation of silica ($\text{SiO}_2\text{-H}_2\text{O}$) nanofluid in an ultrasonic cleaner TJ001. The SiO_2 nanoparticles that used for investigation have an average size of 12 nm and density of 2.65 g/cm^3 . The photographic view of the SiO_2 nanoparticles as seen by the naked eyes is shown in Fig. 2. The SiO_2 nanoparticles with 7.5 g and 15 g are used to prepare 1500 ml of $\text{SiO}_2\text{-H}_2\text{O}$ nanofluid, which corresponds to 0.5% and 1.0% particle mass concentration, respectively. SiO_2 nanoparticles are weighted very accurately using a sensitive balance with a 0.1 mg resolution. The particle mass concentration of $\text{SiO}_2\text{-H}_2\text{O}$ nanofluid in the present study is calculated refer to (1) as [7]:

$$\% \text{ mass concentration} = \frac{W_{\text{SiO}_2}}{W_{\text{bf}}} \times 100 \% \quad (1)$$

where, W_{SiO_2} = Amount of SiO_2 nanoparticles in gram, W_{bf} = Amount of base fluid in gram,

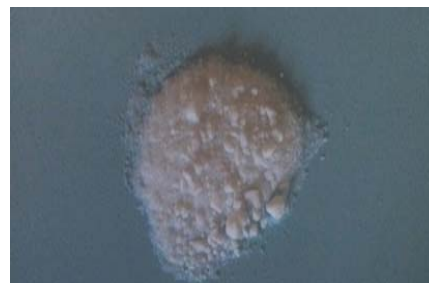


Fig. 2 A photographic view of the SiO_2 nanoparticles

TABLE I
SPECIFICATION OF LHP

Specification	Dimension/Material
Evaporator	
Dimension (mm)	L50 × W50 × H4
Material	Copper
Reservoir	
Volume (Litre)	0.75
Dimension (mm)	L149 × W100 × H85
Sintered Wick	
Pore radius(μm)	1-17
Permeability(m ²)	10 ⁻¹¹ ~10 ⁻¹³
Outer Diameter (mm)	12
Inner Diameter (mm)	10
Material	Nickel
Vapor Line	
Outer Diameter (mm)	15
Inner Diameter (mm)	13.5
Length (mm)	830
Material	Copper
Liquid Line	
Outer Diameter (mm)	15
Inner Diameter (mm)	13.5
Length (mm)	500
Material	Copper
Condenser	
Dimension (mm)	L321 × W100 × H1
Material	Aluminum

C. Thermal Analysis

The objective of the current study is to evaluate the total thermal resistance (R_{th}) of the LHP using SiO₂-H₂O nanofluid as working fluid for various heat inputs under steady state and transient conditions. The results obtained from experimental investigation used to verify by RSM model. The nanoparticle mass concentration that yields the minimum R_{th} is then found out, and the various steps to estimate R_{th} are as follows. The thermal resistance network of the system is shown in Fig. 3.

The heat flux (\dot{q}) that applied on the bottom of base plate can be expressed as:

$$\dot{q} = \frac{Q}{A_b} \quad (2)$$

where Q denotes the heat input and A_b is the area of base plate. The thermal resistances of the LHP are defined as [8]: The thermal resistance between the copper base plate and the evaporator section (R_b) is:

$$R_b = \frac{T_b - T_e}{Q} \quad (3)$$

where T_b denotes the temperature at the copper base plate and T_e is the temperature at the evaporator.

The thermal resistance of the evaporator section (R_e) is:

$$R_e = \frac{T_e - T_v}{Q} \quad (4)$$

where T_v is the temperature at the vapor line.

The thermal resistance of the vapor line (R_v) is:

$$R_v = \frac{T_v - T_c}{Q} \quad (5)$$

where T_c is the temperature at the condenser section.

The convective thermal resistance of the condenser (R_c) is:

$$R_c = \frac{T_c - T_l}{Q} \quad (6)$$

where T_l is the temperature at the liquid line.

The thermal resistance of the liquid line (R_l) is:

$$R_l = \frac{T_l - T_a}{Q} \quad (7)$$

where T_a is the ambient temperature.

According to the thermal resistance network as shown in Fig. 3, the R_{th} of the system is given by:

$$R_{th} = R_b + R_e + R_v + R_c + R_l \quad (8)$$

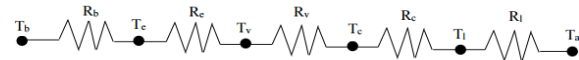


Fig. 3 Thermal resistance network of LHP

III. EXPERIMENTAL DESIGN AND STATISTICAL ANALYSIS

In this study, experimental design of the operating conditions is performed by RSM which is a collection of mathematical and statistical techniques that are useful for the optimization of industrial processes, and widely used for experimental designs [9]. In this study, RSM is used to assess the relationship between response (R_{th}) and operating variables (nanoparticle mass concentration and heat input), in addition to optimize the operating variables to predict the best value of the response. Central Composite Design (CCD), the most commonly used approach of RSM, is utilized in this study. CCD allows reasonable amount of information to test lack of fit when an adequate number of experimental values exist [10]. CCD and RSM are established with the help of the Design-Expert 6.0.7 (Stat-Ease Inc., Minneapolis, MN) software program. The two significant independent variables considered are nanoparticle mass concentration (A) and heat input (B), as presented in Table II. Each independent variable is varied over three levels. The low, center, and high levels of each variable are designated as -1, 0, and +1, respectively. The variable levels are selected based on the results obtained from preliminary experiments.

TABLE II
INDEPENDENT VARIABLES OF THE CCD DESIGN

Level of Value	A Nanoparticle Mass Concentration (%)	B Power Input (W)
-1	0	20
0	0.5	40
1	1.0	60

As there are only three levels for each factor, the appropriate model is an empirical second-order polynomial model (quadratic model) as indicated by Montgomery [11]. The quadratic model used is expressed as:

$$Y = \beta_0 + \sum_{i=1}^k \beta_i x_i + \sum_{i=1}^k \beta_{ii} x_i^2 + \sum_{i=1}^k \sum_{j=1, j \neq i}^k \beta_{ij} x_i x_j + \varepsilon \quad (9)$$

where Y is the predicted response; x_i and x_j are variables or independent factors; β_0 is the constant coefficient; β_i , β_{ij} , and β_{ii} are interaction coefficients of linear, quadratic, and the second-order terms, respectively; k is the number of independent variables (2) and ε is the error [11]. Analysis of variance (ANOVA) is employed for graphical analysis of the data to obtain the interaction between the variables and the response. The quality of the fit polynomial model is expressed by the coefficient of determination (R^2), and its statistical significance is confirmed through the student t test in the same software. Model terms are assessed by the P value (probability) with 95% confidence level. Three-dimensional plots and their particular contour plots are achieved based on effects of the operational variables at three levels.

TABLE III
RESPONSE VALUES FOR DIFFERENT EXPERIMENTAL CONDITIONS

Run No.	Factor A Nanoparticle mass concentration (%)	Factor B Heat input (W)	Response Total thermal resistance (°C/W)
1	0.00	60	2.7998
2	0.50	40	3.2300
3	0.50	40	3.1885
4	0.00	40	3.3010
5	0.50	40	3.2270
6	0.50	20	3.4190
7	0.50	60	2.7054
8	0.50	40	3.1958
9	0.50	40	3.1825
10	0.00	40	3.6890
11	1.00	60	3.6875
12	1.00	20	3.6625
13	1.00	40	2.6645

The total number of experiments for the two factors is obtained as 13. Eight experiments are enhanced with five replications to assess the pure error. A total of 13 runs of the CCD experimental design and response are illustrated in Table III which illustrates the outcome of the experimental conditions as average of the triplicate tests achieved for each operating condition.

IV. RESULTS AND DISCUSSION

A. Effects of Nanoparticle Mass Concentration and Heat Input on R_{th}

Fig. 4 shows the relationship between the R_{th} and nanoparticle mass concentration for various heat input. As depicted in Fig. 4, the R_{th} decreased up to 0.5% and increased on further increase in nanoparticle mass concentration (from 0.5% to 1%) at all heat inputs. Thus, there is an optimal

particle concentration, which is about 0.5% for the SiO₂-H₂O-charged LHP in the present experiment. Thus, the addition of silica nanoparticles to base water with high mass concentration deteriorated the thermal performance of the LHP due to the depositions with larger particle agglomerates appeared at the evaporator as reported by Qu and Wu [12]. At the optimal mass concentration of 0.5%, the maximum reduction in R_{th} of SiO₂-H₂O-charged LHP is about 2.702 °C/W (or 5.5%) under heat input of 60W, is obtained as compared with pure water (0% nanoparticle mass concentration) charged LHP. It is clear from the Fig. 4 that when the heat input increases, the thermal resistance decreases and the nanoparticle mass concentration has a great impact on the R_{th} . Table IV summarizes the changes in R_{th} with nanoparticle mass concentration and heat input.

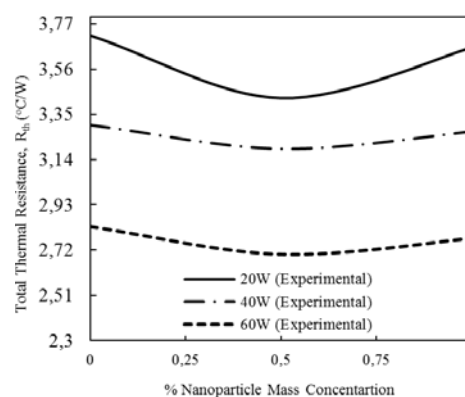


Fig. 4 Influence of nanoparticle mas concentrations on the R_{th} of LHP for various heat inputs

TABLE IV
SUMMARY OF R_{th} AT VARIOUS NANOPARTICLE MASS CONCENTRATIONS AND HEAT INPUTS

Q (W)	R_{th}		
	0%	0.50%	1%
20	3.716	3.425	3.660
40	3.311	3.191	3.270
60	2.859	2.702	2.775

TABLE V
ANNOVA FOR ANALYSIS OF VARIANCE AND ADEQUACY OF THE QUADRATIC MODEL

Source	Sum of squares	d.f	Mean square	F Value	P>F
Model	1.16	5	0.23	75.65	<0.0001
A	5.01E-003	1	5.010E-003	1.63	0.0142
B	1.11	1	1.11	360.06	<0.0001
A ²	0.035	1	0.035	11.27	0.0121
B ²	0.033	1	0.033	10.76	0.0135
AB	1.842E-003	1	1.842E-003	0.60	0.4644
Residual	0.022	7	3.076E-003		
Lack of Fit	0.020	3	6.520E-003	13.22	0.5152
Pure Error	1.973E-003	4	4.932E-004		

SD = 0.055, mean = 3.20, CV = 1.74, $R^2 = 0.9818$, $R^2_{adj} = 0.9689$, Adeq. Precision = 25.977.

A. Analysis of Variance

Table V demonstrates the ANOVA of regression parameters of the predicted response surface quadratic model.

The model for R_{th} is found to be significant using the t test at 5% significance level ($P < 0.05$). The F value of 75.65 of the model and its low probability value indicate that the model is significant for R_{th} ($F > 0.10$ shows that the model terms are insignificant).

As shown in Table V, the “Adequate Precision” ratio of the model is 25.977 (Adequate Precision > 4), which is an adequate signal for the model [13]. The value of coefficient of determination ($R^2 = 0.9818$) obtained for R_{th} is above 0.80, showing that only 1.82% ($1 - 0.9818$) of the total dissimilarity might not be explained by the empirical model. For a high-quality fit of a model, the coefficient of determination should be more than 0.80 [11]. High R^2 value demonstrates excellent conformity between the calculated and observed results within the range of experiment. In this study, A , B , A^2 , and B^2 are significant model terms. Insignificant model terms’ limited weights, such as AB , are excluded from the study in order to get better model [11]. The response surface model created for predicting R_{th} has been considered sensible. The final regression model, in terms coded factors, is expressed by the following second-Order Polynomial Equation:

$$R_{th} = +3.71472 - 0.42017A + 0.00148548B + 0.44821A^2 - 0.000273681B^2 \quad (10)$$

By concerning the diagnostic plots provided by the software, such as normal probability plots of the student zed residuals, as well as the predicted versus actual value plots, the model validity could be judged. Fig. 5 shows the normal probability plots of the studentized residuals for R_{th} . A normal probability plot demonstrates whether the residuals follow a normal distribution; in this case, it can be assumed that the data is normally distributed. The assessment of actual and predicted values of R_{th} is shown in Fig. 6. Actual values are the measured response data for a particular run, and the predicted values are evaluated from the model and generated by using the approximating functions. The agreement between the actual and predicted values of R_{th} is satisfactory and in agreement with the statistical significance of the quadratic model presented in Table IV.

B. Interaction between Variables and Optimization

Equation (10) is used to visualize the influences of operating variables (i.e., nanoparticle mass concentration and heat input) on R_{th} (Fig. 7). The curvature of 3D surfaces indicates that the nanoparticle mass concentration and heat input have major effect on R_{th} ; increasing the nanoparticle mass concentration up to about 0.5% leads to decrease in R_{th} and then begins to increase, while the increasing of the heat input also leads to significant decrease in R_{th} .

The results are optimized via Design-Expert software. In numerical optimization, nanoparticle mass concentration and heat input are goaled to be in range, R_{th} was aimed to be minimized. At the optimized conditions, nanoparticle mass concentration of 0.48% and heat input of 59.97W, R_{th} being 2.66°C/W which is predicted based on desirability function of 1.00. To verify the accuracy of the predicted model and the

consistency of the optimum combination, an additional run is conducted under optimal conditions based on the results from the model. The results show that the model prediction for the R_{th} is very close to the actual experimental results (Table IV). These results confirm that RSM is a powerful tool for optimizing the operational conditions for minimum R_{th} of LHPs.

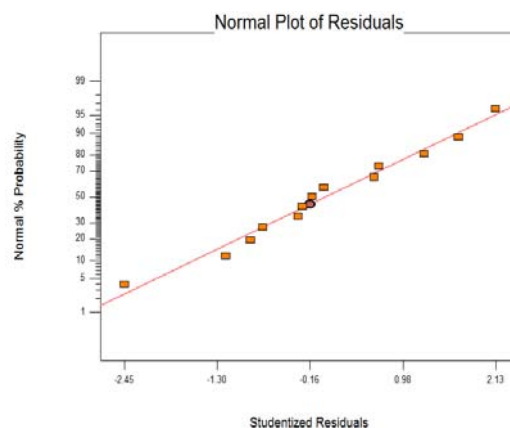


Fig. 5 Normal probability plot of studentized residuals

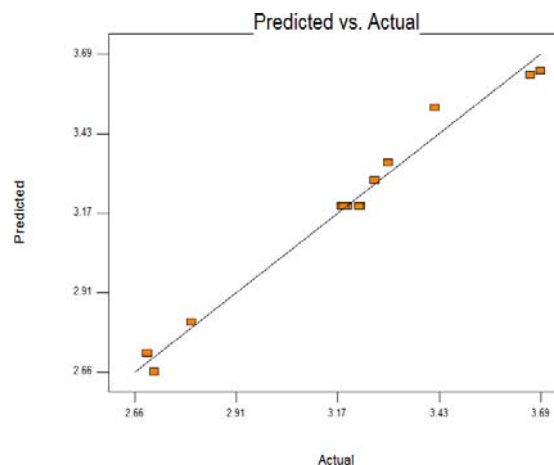


Fig. 6 Predicted versus actual values of R_{th}

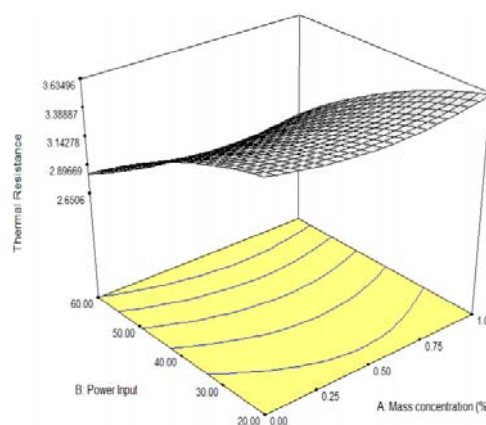


Fig. 7 3D surface plots of R_{th} as function of nanoparticle mass concentration (A) and heat input (B)

V.CONCLUSION

The experimental design and optimization of operating conditions of LHP for desktop PC cooling is accomplished with RSM. The independent variables are nanoparticle mass concentration and heat input, and the objective function is total thermal resistance (to minimize). Results show that the nanoparticle mass concentration and the heat input are crucial on the R_{th} . The results are optimized via Design-Expert software and found that a nanoparticle mass concentration of 0.48% and heat input of 59.97W could produce the minimum R_{th} (2.66°C/W). This study may be extended for more variables such as other types of nanoparticles mass concentration and geometrical parameters such as the diameter and the length of LHP in designing efficient nanofluid-charged LHPs.

ACKNOWLEDGMENT

The authors would like to sincerely thank the Ministry of Higher Education (MOHE) of Malaysia for the provision of a grant with code no. 20120228FRGS to support this work.

REFERENCES

- [1] D. X. Gai, Z. C. Liu, W. Liu, and J. G. Yang, "Operational characteristics of miniature loop heat pipe with flat evaporator," *Heat and Mass Transfer*, vol. 46, pp. 267-275, 2009.
- [2] Yu. F. Maydanik, "Loop heat pipes," *Applied Thermal Engineering*, vol. 25, pp. 635-657, 2005.
- [3] S. U. S. Choi, "Enhancing thermal conductivity of fluids with nanoparticles," in *Developments Applications of Non-Newtonian Flows*, FED-vol. 231/MD-vol. 66, ASME: 99-105, edited by D. A. Siginer and H. P. Wang, New York, 1995.
- [4] M. Shafahi, V. Bianco, K. Vafai, and O. Manca, "Thermal performance of flat-shaped heat pipes using nanofluids," *Int. J. Heat Mass Transfer*, vol. 53, pp. 1438-1445, 2010.
- [5] M. Shafahi, V. Bianco, K. Vafai, and O. Manca, "An investigation of the thermal performance of cylindrical heat pipes using nanofluids," *Int. J. Heat Mass Transfer*, vol. 53, pp. 376-383, 2010.
- [6] K. H. Do and S. P. Jang, "Effect of nanofluids on the thermal performance of a flat micro heat pipe with a rectangular grooved wick," *Int. J. Heat Mass Transfer*, vol. 53, pp. 2183-2192, 2010.
- [7] P. Naphon, D. Thongkum, and P. Assadamongkol, "Heat pipe efficiency enhancement with refrigerant-nanoparticles mixtures," *Energy Conversion and Management*, vol. 50, pp. 772-776, 2009.
- [8] G. Franchi and X. Huang, "Development of Composite Wicks for Heat Pipe Performance Enhancement," *Heat Transfer Engineering*, vol. 29 (10), pp. 873-884, 2008.
- [9] D. Bas and I. H. Boyaci, "Modeling and optimization in usability of Response Surface Methodology (RSM)," *Journal of Food Engineering*, vol. 78, pp. 836-845, 2007.
- [10] M. J. K. Bashir, H. A. Aziz, M. S. Yusoff, and M. N. Adlan, "Application of Response Surface Methodology (RSM) for optimization of Ammoniacal Nitrogen removal from semi-aerobic landfill leachate using ion exchange resin," *Desalination*, vol. 254, pp. 154-161, 2010.
- [11] D. C. Montgomery, "Design and analysis of experiments," 7th Edition, John Wiley & Sons, Inc., New York, 2008.
- [12] J. Qu and H. Wu, "Thermal performance comparison of oscillating heat pipes with SiO₂/water and Al₂O₃/water nanofluids," *International Journal of Thermal Sciences*, vol. 50, pp. 1954-1962, 2011.
- [13] Design-Expert Software Trial Version 6.0.7, User's guide, 2008.